Academic Science Journal

Sensorial Behavior of Polypyrrole Nanofibers Prepared by Chemical Oxidative Polymerization

Omar A. Hussein*, T. H. Mubarak and Isam M. Ibrahim

Departments of Physics – College of science – University of Diyala

omarah10@yahoo.com

Received: 1 July 2022 **Accepted: 3 September 2022**

DOI: https://dx.doi.org/10.24237/ASJ.01.02.626C

Abstract

Conductive polymer (CPs) materials include polypyrrole nanofibers (PPy-NFs). The chemical oxidation of pyrrole monomer with Iron (III) chloride in the presence of methyl orange at 3 ^{0}C had synthesized polypyrrole nanofibers (PPy-NFs). Polypyrrole nanofibers (PPy-NFs) were determined to be amorphous, based on the XRD spectra. According to the TEM test, PPy is polymerized into one-dimensional nanofibers with a nanofibers structure that has distinct diameters with widths varying from (50-100 nm). The PPy-NFs in the manufactured nanostructures were investigated using RAMAN to identify their composition. Additionally, The NH_3 gas- sensing performance of the PPy NFs thin films for the prepared molar ratio was tested.

Keywords: Conductive polymer, Polypyrrole nanofibers, TEM, gas sensor.

Academic Science Journal

السلوك التحسسي للألياف النانوية لبوليمر البولي بايرول المحضرة عن طريق البلمرة الكيميائية المؤكسدة

عمر احمد حسين, عصام محمد ابراهيم, تحسين حسين مبارك

قسم الفيزياء – كلية العلوم – جامعة ديالى

الخلاصة

ركز هذا العمل على تحضير ألياف نانوية لبوليمر البولي بايرول (PPy-NFs) بتقنية البلمرة الكيميائية عن طريق الأكسدة الكيميائية لمونومر البيرول مع كلوريد الحديد (III) بوجود برتقالي الميثيل عند درجة حرارة($3\ ^0C$), تمت دراسة المادة المحضرة وتشخيصها باستخدام العديد من التقنيات ومنها تقنية حيود الاشعة السينية (XRD) ومطيافية رامان والمجهر الالكتروني النافذ (TEM). حيث بينت نتائج (XRD) الطابع غير المتبلور للبولي بايرول بينما أكد فحص رامان تكوين البوليمر, كذلك تمت بلمرة بوليمر البولي بيرول إلى ألياف نانوية أحادية البعد ذات أقطار مميزة (100nm-50) وفقا لاختبار (TEM). بالإضافة إلى ذلك, تم اختبار أداء استشعار غاز الامونيا للأغشية الرقيقة المصنعة من الالياف البوليميرية المحضرة.

الكلمات المفتاحية: البوليمر الموصل, الالياف النانوية للبولي بايرول, المجهر الالكتروني النافذ, المتحسس الغازي.

Introduction

Conductive polymers (CPs) have shown great potential in recent years as materials for chemical-sensing, light-emitting electronic instruments, separation membranes, and antistatic coatings because of their metallic conductivity, ease of turning between redox states, lower cost, ease of synthesis, and the ability to be produced in large quantities to meet specific requirements [1-4]. The synthesis of materials of decreased dimensions, such as balls, tubes, wires, fibers, particles, and thin films, has recently attracted more attention. These materials can display characteristics that are noticeably different from those of bulk conductive polymeric materials [5,6]. One-dimensional conductive polymer nanostructures particularly

have drawn a lot of technological and academic attention due to the possibility of using them as materials for molecular fibers or wires. To date, electrochemical fabrication, template method, seeded polymerizations, and interfacial polymerization have all been used to synthesize conductive polymer materials having one-dimensional nanostructures, such as polyaniline, polypyrrole, polythiophene, and its derivatives [7,8]. Therefore, producing conductive polymer nanostructures on a wide scale with regulated morphology and size continues to be an exciting challenge for researchers. Due to their built-in electrical, optical, and mechanical transduction mechanisms, conductive polymers could be incorporated into sensors to identify specific analytes [9]. Furthermore, metal oxide or carbon-based sensing typically functions at high temperatures to generate quick and detectable responses [10], in contrast to the conducting polymer-based gas sensors, which can achieve adequate efficiency for some analytes at room temp [11]. To reveal chemical and biological species, a variety of conductive polymers have been used extensively [12,13]. For example, a variety of Polyaniline nanofibers have been used to identify bases, acids, and organic vapors [14]. In this paper, we present a simple and effective approach for synthesizing polypyrrole nanofibers on a large scale. Polypyrrole nanofibers are described using X-ray diffraction (XRD), transmission electron microscopy (TEM), and the RAMAN test. The electrical response of PPy-NFs to ammonia exposure was tested to demonstrate its sensing capabilities.

Experimental work

Synthesis of PPy nanofibers (PPy-NFs)

Throughout the method, 2.5 mM (0.08185 g) methyl orange (MO) (LTD Rubilabor Chemical Co. Spain) was dissolved in de-ionized water (288 ml) and mixed with (14 mM) pyrrole monomer (Sigma Aldrich, China) to create a (Pyrrole monomer- methyl orange) solution, which was then iced to 3^{o}C through the use of an ice bath. For 10 minutes, the mixture was dynamically agitated until all agglomerates had vanished. In 33 ml de-ionized water, 1.702 (10mM) ($FeCl_3$) (AlPHA chemica) was dissolved. Then, over two hours, it was dripped into the (Py-MO) solution. In ice baths, these reaction solutions were agitated for 24 hours. To

separate the remaining contaminants (impurities) in PPy-NFs, the precipitated PPy-NFs were filtered and rinsed three times with acetone, alcohol, and water. Finally, the product was dried in an oven for six hours at 75 ° C.

System of gas sensors

Figure 1 shows the setup of the testing equipment, which includes a schematic design of the electrical circuit for gas sensing measurements. To make consistent solutions, specific amounts of the sample powder were dissolved in distilled water and ultrasonic for 90 minutes. After choosing an appropriate mask to make the gold track to the electrode, these solutions were spin-coated on the silicon substrate, and molten gold was sprayed on the sample film by a nozzle with a specific spraying time. The size of the gas sensor device was (1cm ×1cm).

In the gas sensing system, the gas sensor was placed inside a cylindrical steel chamber, with two pins of metal electrodes contacting the gas sensor's gold electrodes to record the electrical resistance when the surface sample was exposed to air. The chamber was then sealed and the rotary pump was turned on to reduce the pressure inside the chamber to around 1 m bar. When a surface sample is exposed to ammonia gas with consistent periods of ON and OFF gas exposure, the electrometer records the change in electrical resistance as a function of time.

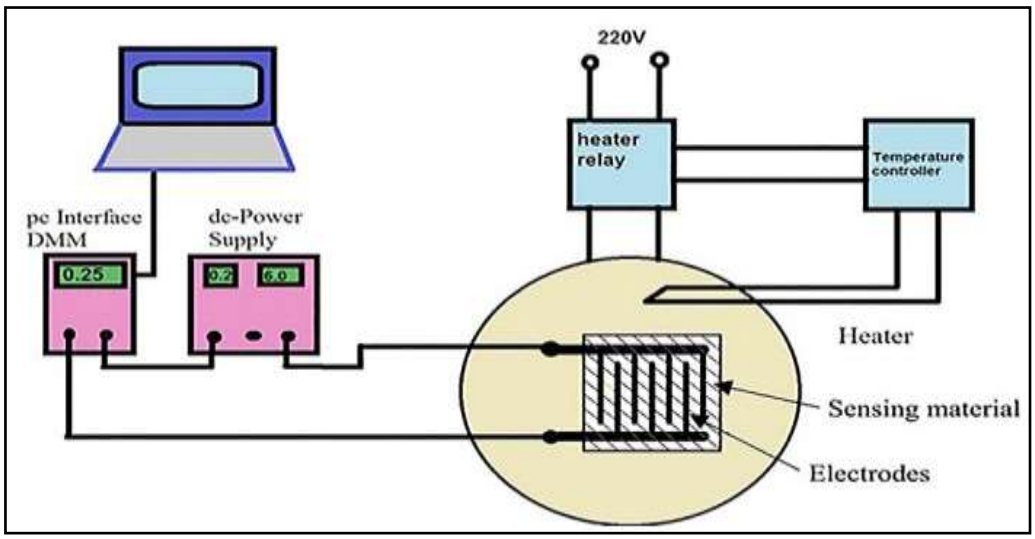

Figure 1: Electric circuit setup of the gas sensor [15].

Academic Science Journal

Results and Discussion

X-ray diffraction measurements

The crystal structure of PPy-NFs samples was studied using an X-ray diffractometer (XRD) to characterize the phase content of the samples.

The XRD patterns of PPy-NFs are shown in Figure 2. The PPy-NFs powder is amorphous in form, meaning it is a non-crystalline solid with atom distribution that does not follow any crystalline structure, according to X-ray diffraction tests. The wide peak was caused by X-rays diffusing from the PPy-NFs chain. A broad peak can be seen in Fig. 1 at roughly 2 = 24.5°, which is assigned to the (102) directions [16]. Amorphous PPy is distinguished for its broad peak. A broad halo pattern in the ranges 2 = 10 - 35 is attributed to PPy-NFs formed by oxidative polymerization and is typical of polypyrrole doped structures (17, 18). According to equation (1) that calculated the average chain separation (S) which calculates to be 4.53Å for polypyrrole nanofibers.

$$S=5\lambda/8\sin\theta \quad \text{..... (1)}$$

Here, λ and θ stand for the X-ray wavelengths and the diffraction angles at peaks of the amorphous Halo (19, 20) respectively.

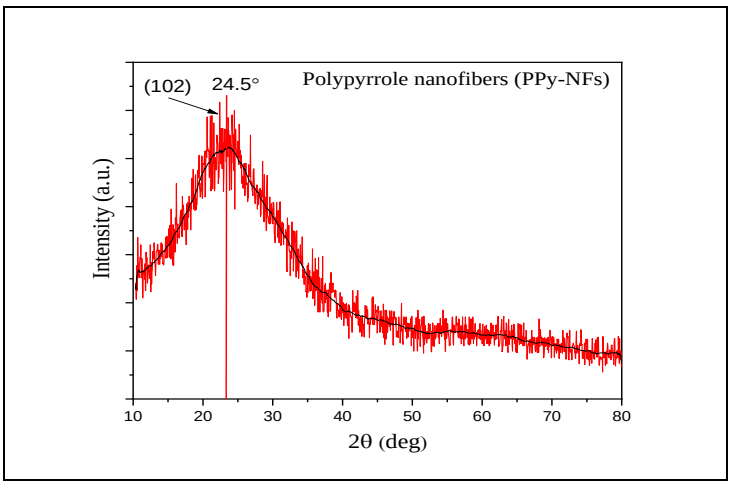

Figure 2: XRD pattern of (PPy-NFs).

TEM image analysis of PPy-NFs

A typical TEM image of PPy nanomaterials produced in an ice bath *is* shown in Figure 3. The TEM image revealed that the final product was entirely made up of a random network of texture nanofibers with widths ranging from ≈ (50-100) nm. Furthermore, the fibers tended to agglomerate together into interconnected networks as arbitrary nanofibrous mat, making determining the exact length of the fibers challenging. The TEM scan also demonstrated that these fibers were solid, not hollow, indicating that one-dimensional (1D) nanofibers had formed.

The fibrillar morphology of these PPy samples could be caused by the following hypothesis: To begin with, the restricted availability of both hydrophobic and hydrophilic regions at the interface resulted in 1D growth and sideway aggregation inhibition. Second, the polymerization time was kept to a minimum, allowing for the formation of ordered and integrated structures. This also allowed for the avoidance of the PPy material's side chain formation shortcomings. Third, when substantial dopants were utilized, regularity in the PPy backbone was improved due to the prevention of side effects (reactions) [21].

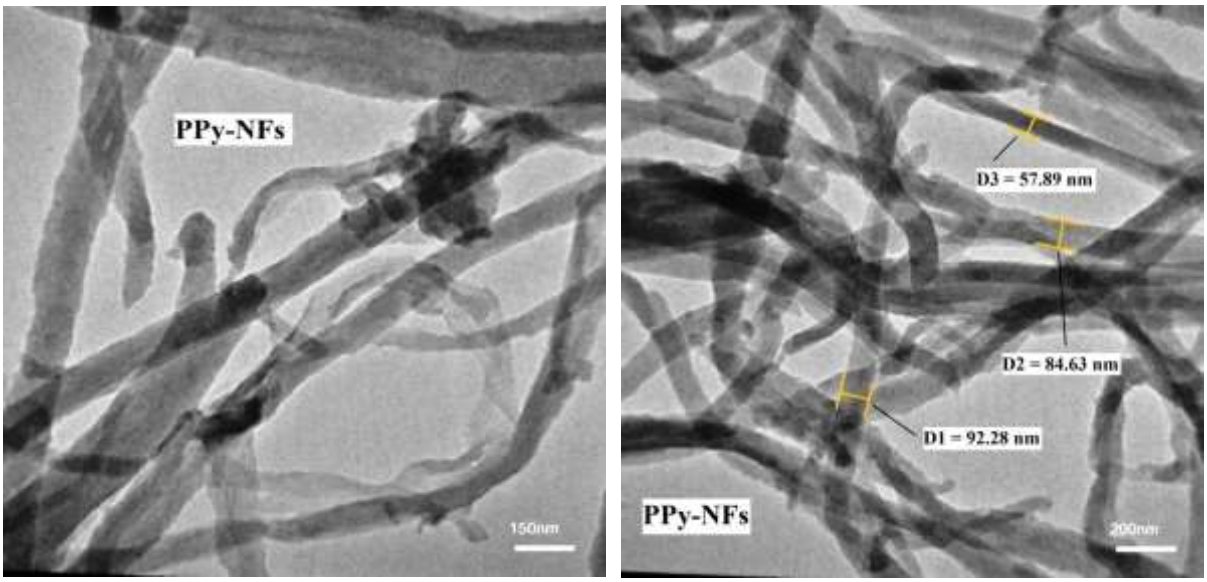

Figure 3: TEM images of PPy-NFs at different magnification.

Academic Science Journal

RAMAN spectroscopy analysis of PPy-NFs

The composition of the PPy nanofibers was further confirmed using the Raman spectrum. The characteristic bands were observed at 1370 cm^{-1} and 1564 cm^{-1} due to the ring stretching mode and the C=C backbone stretching of PPy, respectively. In addition, the peaks obtained at 936 cm^{-1} and 1052 cm^{-1} were attributed to the bipolaron ring deformation and the polaron symmetric C–H inplane bending vibration, respectively. The RAMAN bands in Figure 4 were in good agreement with those described in the literature for polypyrrole [22, 23]. The Raman peaks shown in Figure 4 are summarized in table 1, including the assigned predominant band vibrations.

Table 1: Raman peaks for PPy-NFs.

Band code	Wavenumber (cm^{-1})	Band Type
1	623	C–C ring-torsional
2	688	C–H wagging
3	936	C–C ring-deformation (bipolarons)
4	1052	C–H in plane-deformation (polarons)
5	1370-1384	C–C in-ring, C–H bending, antisymmetric C–N stretching and N–H bendin stretching
6	1564	C=C backbone stretching peak of polypyrrole

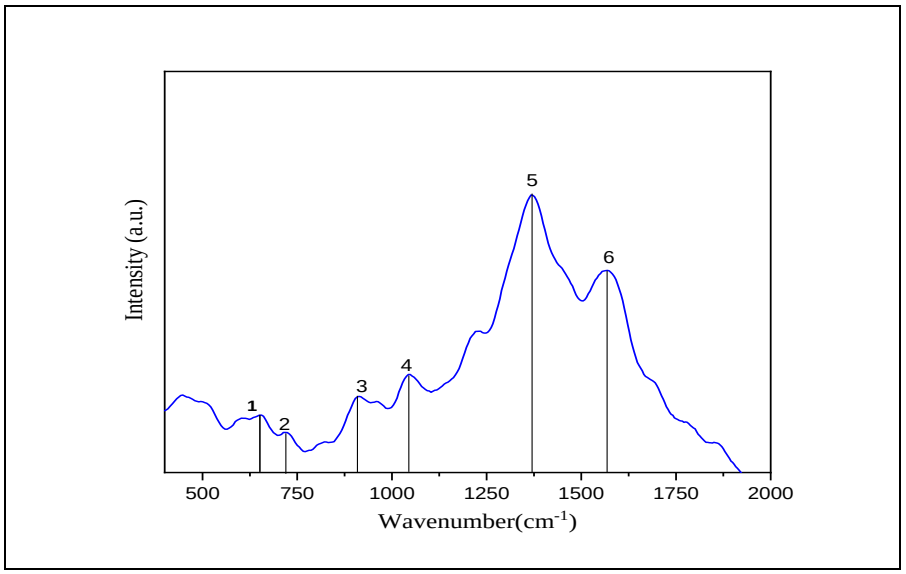

Figure 4: Raman spectra for the PPy-NFs

Ammonia gas sensing measurement

Polypyrrole has been used to study ammonia sensing in the laboratory. The interaction of Polypyrrole nanofibers with ammonia gas caused a change in resistance (conductivity), which was followed by the return to the original state when exposed to air. The following reasonable method can be used to depict the entire process of reversible reactions.

$$PPyH^{+} + NH_3 \longleftrightarrow PPy + NH_4 \quad \text{.....(2)}$$

$$PPy + NH4^{+} \xrightarrow{\text{Moist Air}} PPyH^{+} + NH_3 + H_3O^{+} \quad \text{..... (3)}$$

Sensitivity is defined by the resistance change when the sensor is exposed to a certain concentration of gas [24].

The sensitivity can be calculated as:

$$S = \left|\frac{R_g - R_a}{R_a}\right| \times 100\% \quad \text{..... (4)}$$

Where S is the sensitivity, R_a and R_g are the electrical resistance of the film in the air and the electrical resistance of the film in the presence of gas, respectively.

Ammonia is an odorless, colorless gas or compressed liquid. It is one of the most harmful and toxic gases, damaging the lungs, skin, and eyes. Ammonia concentrations in the human body of up to 500 parts per million (ppm) can be exceedingly hazardous. They can cause pulmonary oedema, or the collection of fluid in the lungs, at 1000 parts per million. At low ppm concentrations, the human nose has difficulty detecting ammonia. VOC gases such as liquid ammonia have piqued the interest of researchers since they not only pollute the environment but also have a direct influence on human health. Regardless, these gases are used in the production of other products that are strongly tied to human life [25]. The presence of such hazardous VOCs is very likely, necessitating the development of sensors to identify poisonous and combustible chemicals early on. Nanomaterials with the right size,

dimension, and shape show a lot of promise for sensing applications. Gas sensor performance is influenced by humidity, working temperature, and gas concentration. Features connected with materials morphologies, like the contact area, the specific surface area, the grain size, the porosity, the grain stacking order, and aggregation, are influencing factors in addition to external influences.

The reactions of PPy-NFs to NH_3 exposure at 500C with 30 ppm are shown in Figure 5. It is commonly known that PPy is a p-type conducting semiconductor. When PPy is exposed to an electron donor gas, such as NH_3, it undergoes a redox process [15]. When NH_3 is added to PPy, the charge-carrier concentration of the polymer drops, and neutral polymer backbones form. When PPy-NFs were exposed to NH_3 vapor for 39.2 seconds, the resistance increased dramatically. As a result, PPy-NFs made this way have a characteristic nanofiber morphology and perform better in terms of sensitivity and response time [26]. The values of the responsivity, response time and recovery time for PPy-NFs were listed in Table 2.

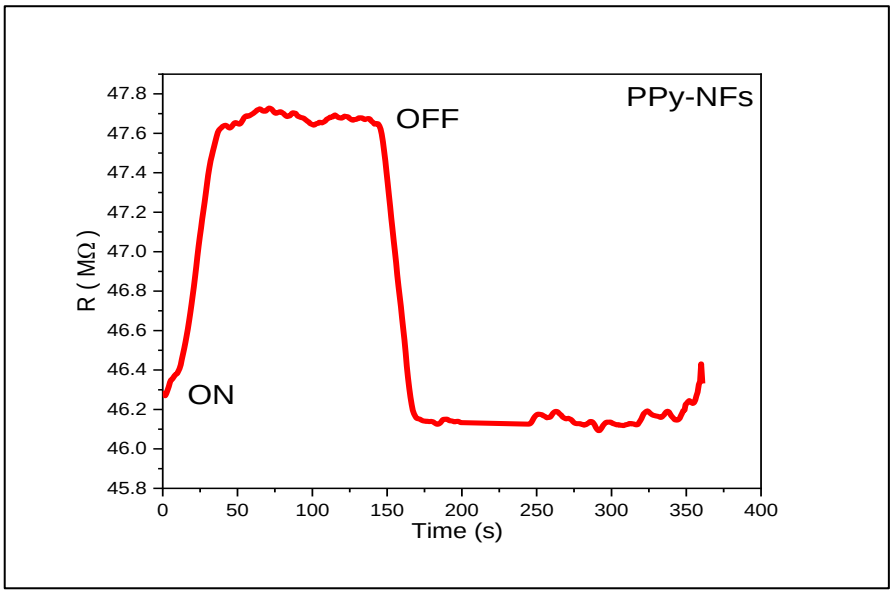

Figure 5: Variation of resistance with time for PPy-NFs sensor.

Table 2: The responsivity, response time and recovery time for PPy-NFs sample at 50°C with 30 ppm of NH_3 gas concentration.

Sample	Responsivity %	Response time (s)	Recovery time (s)
Polypyrrole nanofibers	3.01	34.2	25.6

Conclusions

Here, we will concentrate on the key conclusions of the study process, which is that chemical oxidative polymerization was used to create polypyrrole nanofibers (PPy-NFs), which is a simple and feasible method. Polypyrrole nanofibers (PPy-NFs) are amorphous according to XRD spectra. In addition, The RAMAN spectra analyses confirmed forms of PPy-NFs. FESEM images demonstrated that the Polypyrrole was polymerized in one dimension nanofibers materials. Finally, the polypyrrole nanofibers (PPy-NFs) were used as the chemical sensing element in the sensor device to detect ammonia gas. The responsivity, response time and recovery time for PPy-NFs sample were measured and their values were 3.01%, 34.2 sec, and 25.6 sec, respectively.

References

1. A. Rahy, M. Sakrout, S. Manohar, S. J. Cho, J. Ferraris, D. J. Yang, Chemistry of Materials, 20(15), 4808-4814(2008)
2. M. C. Kum, K. A. Joshi, W. Chen, N. V. Myung, A. Mulchandani, Talanta, 74(3), 370-375(2007)
3. S. Manigandan, S. Majumder, S. Ganguly, K. Kargupta, Materials Letters, 62(17-18), 2758-2761(2008)
4. G. Sonmez, Chemical communications, (42), 5251-5259(2005)
5. L. Li, Y. Huang, G. Yan, F. Liu, Z. Huang, Z. Ma, Materials Letters, 63(1), 8-10(2009)
6. A. Kros, N. A. Sommerdijk, R. J. Nolte, Sensors and Actuators B: Chemical, 106(1), 289-295(2005)
7. C. R. Martin, Chemistry of materials, 8(8), 1739-1746(1996)
8. X. Yang, Z. Zhu, T. Dai, Y. Lu, Macromolecular rapid communications, 26(21), 1736-1740(2005)
9. E. S. Forzani, H. Zhang, L. A. Nagahara, I. Amlani, R. Tsui, N. Tao, Nano Letters, 4(9), 1785-1788(2004)
10. J. F. Liu, X. Wang, Q. Peng, Y. Li, Advanced Materials, 17(6), 764-767(2005)

11. J. Janata, M. Josowicz, Nature materials, 2(1), 19-24(2003)
12. Q. Ameer, S. B. Adeloju, Sensors and Actuators B: Chemical, 106(2), 541-552(2005)
13. S. Carquigny, J. B. Sanchez, F. Berger, B. Lakard, F. Lallemand, Talanta, 78(1), 199-206(2009)
14. S. Virji, J. D. Fowler, C. O. Baker, J. Huang, R. B. Kaner, B. H. Weiller, Small, 1(6), 624-627(2005)
15. A. H. Omar, Synthesis and Characterization of (Polypyrrole-Ferrites) Nanocomposites for Multi-Applications, PH. D. Thesis, University of Diyala, Iraq, (2022)
16. E. A. Sanches, S. F. Alves, J. C. Soares, A. M. da Silva, C. G. da Silva, S. M. de Souza, H. O. da Frota, Journal of Nanomaterials, (2015)
17. C. MA, P. SG, G. PR, S. Shashwati, P. VB, Soft nanoscience letters, (2011)
18. C. K. Ong, S. Ray, R. P. Cooney, N. R. Edmonds, A. J. Easteal, Journal of applied polymer science, 110(1), 632-640(2008)
19. K. Cheah, M. Forsyth, V.-T. Truong, Synthetic metals, 94(2), 215-219(1998)
20. J. Ouyang, Y. Li, Polymer, 38(15), 3997-3999(1997)
21. S. Goel, N. A. Mazumdar, A. Gupta, Polymers for Advanced Technologies, 21(3), 205-210(2010)
22. M. Šetka, R. Calavia, L. Vojkůvka, E. Llobet, J. Drbohlavova, S.Vallejos, Scientific reports, 9(1), 1-10(2019)
23. X. Li, D. Fang, Y. Cao, Z. Luo, M. Jiang, W. Xu, C. Xiong, Journal of Materials Science, 51(20), 9526-9533(2016)
24. R. Garg, V. Kumar, D. Kumar, S. K. Chakarvarti, J. Sensors Instrum., 3(1), 1-13(2015)
25. S. D. Raut, V. V. Awasarmol, B. G. Ghule, S. F. Shaikh, S. K. Gore, R. P. Sharma, R. S. Mane, Materials Research Express, 5(6), 065035(2018)
26. X. Yang, L. Li, Synthetic metals, 160(11-12), 1365-1367(2010)